Feedback Control Law for Variable Speed Control Moment Gyros

Hanspeter Schaub , Srinivas R. Vadali and John L. Junkins

Simulated Reprint from

Journal of the Astronautical Sciences

Vol. 46, No. 3, July–Sept., 1998, Pages 307–328

A publication of the
American Astronautical Society
AAS Publications Office
P.O. Box 28130
San Diego, CA 92198

Journal of the Astronautical Sciences Vol. 46, No. 3, July–Sept., 1998, Pages 307–328

Feedback Control Law for Variable Speed Control Moment Gyros

Hanspeter Schaub*, **Srinivas R. Vadali**† and **John L. Junkins**‡

Abstract

Variable speed control moment gyroscopes are single-gimbal gyroscopes where the fly wheel speed is allowed to be variable. The equations of motion of a generic rigid body with several such variable speed CMGs attached. The formulation is such that it can easily accommodate the classical cases of having either control moment gyros or reaction wheels to control the spacecraft attitude. A globally asymptotically stabilizing nonlinear feedback control law is presented. For a redundant control system, a weighted minimum norm inverse is used to determine the control vector. This approach allows the variable speed control moment gyroscopes to behave either more like classical reaction wheels or more like control moment gyroscopes, depending on the local optimal steering logic. Where classical control moment gyroscope control laws have to deal with singular gimbal angle configurations, the variable speed control moment gyroscopes are shown not to encounter any singularities for many representative examples considered. Both a gimbal angle velocity and an acceleration based steering law are presented. Further, the use of the variable speed CMG null motion is discussed to reconfigure the gimbal angles to preferred sets. Having a variable reaction wheel speed allows for a more general redistribution of the internal momentum vector.

Introduction

Instead of using thrusters to perform precise spacecraft attitude maneuvers, usually control moment gyros (CMGs) or reaction wheels (RWs) are used. A single-gimbal CMG contains a wheel spinning at a constant rate. To exert a torque onto the spacecraft this wheel is gimbaled or rotated about a body-fixed axis.[1, 2, 3] The rotation axis and rotation angle are referred to as the gimbal axis and gimbal angle respectively. A separate feedback control loop is used to spin up the rotor to the required spin rate and maintain it. The advantage of a CMG is that a relatively small gimbal torque input is required to produce a large effective torque output on the spacecraft. This makes a cluster of CMGs a very popular choice for reorienting large space structures such as the space station or Skylab. The drawback of the single-gimbal CMGs is that their control laws can be fairly complex and that such CMG systems encounter certain singular gimbal angle configurations. At these singular configurations the CMG cluster is unable to produce the required torque exactly, or any torque at all if the required torque is orthogonal to the plane of allowable torques. Several papers deal with this issue and present various solutions.[4, 1, 2, 3] However, even with singularity robust steering laws or when various singularity avoidance strategies are applied, the actual torque produced by the CMG cluster is never equal to the required torque when maneuvering in the proximity of a singularity.

*Graduate Research Assistant, Aerospace Engineering Department, Texas A&M University, College Station TX 77843.
†Professor, Department of Aerospace Engineering, Texas A&M University, College Station, TX 77843.
‡George J. Eppright Distinguished Chair Professor of Aerospace Engineering, Aerospace Engineering Department, Texas A&M University, College Station TX 77843, Fellow AAS.

The resulting motion may be stable, but these path deviations can be highly undesirable in some applications.

Reaction wheels (RWs), on the other hand, have a wheel spinning about a body fixed axis whose spin speed is variable. Torques are produced on the spacecraft by accelerating or decelerating the reaction wheels.[5,6] RW systems don't have singular configurations and typically have simpler control laws than CMG clusters. Drawbacks to the reaction wheels include a relatively small effective torque being produced on the spacecraft and the possibility of reaction wheel saturation. To exert a given torque onto a spacecraft, reaction wheels typically require more energy than CMGs.

Variable Speed Control Moment Gyroscopes (VSCMGs) combine positive features of both the single-gimbal CMGs and the RWs. The spinning disk can be rotated or gimbaled about a single body fixed axis, while the disk spin rate is also free to be controlled.[7] This adds an extra degree of control to the classical single-gimbal CMG device. Note that adding this variable speed feature would not require the single-gimbal CMG to be completely reengineered. These devices already have a separate feedback loop that maintains a constant spin rate. What might need to be changed is the torque motor controlling the RW spin rate, which would need to be stronger, and the constant speed RW feedback law, which would be abandoned. With this extra control, singular configurations, in the classical CMG sense, will not be present. Because CMGs are known to be more efficient energy wise than RWs, away from a classical single-gimbal CMG singular configuration, the VSCMG steering law will ideally act like the classical CMG steering law. As a single-gimbal CMG singularity is approached, the VSCMGs should begin to act more like RWs to avoid the excessive torques that would normally occur and ensure that the applied torque of the VSCMG cluster is exactly equal to the required torque. This strategy will allow for precise steering without path deviations near classical CMG singularities because the actual commanded torque will be generated at all times. In this paper, both a gimbal velocity based and an gimbal acceleration based steering law will be presented. Lyapunov analysis will be used to guarantee global asymptotic stability of the feedback control law. Further, the use of the VSCMG null motion to reconfigure the gimbal angles and modify the RW spin speed is discussed. Having a variable speed RW allows for this to be done in a much more general manner. The torque required of these types of maneuvers and whether they could be done with existing CMG hardware will be investigated.

Equations of Motion

To simplify the development and notation, the rotational equations of motion are first derived for the case where only one VSCMG is attached to a rigid spacecraft. Afterwards, the result is expanded to incorporate a system of N VSCMGs. Let $\mathcal{G}$ be the gimbal reference frame whose orientation is given by the triad of unit vectors $\{\hat{\boldsymbol{g}}_s, \hat{\boldsymbol{g}}_t, \hat{\boldsymbol{g}}_g\}$ as shown in Figure 1. The vector components of the unit vectors $\hat{\boldsymbol{g}}_i$ are assumed to be given in the spacecraft reference frame $\mathcal{B}$. Note that because the VSCMG gimbal axis $\hat{\boldsymbol{g}}_g$ is fixed relative to $\mathcal{B}$, only the orientation of the spin axis $\hat{\boldsymbol{g}}_s$ and the transverse axis $\hat{\boldsymbol{g}}_t$ will be time varying as seen from the $\mathcal{B}$ frame. Given an initial gimbal angle γ_0, the spin and transverse axis at a gimbal angle $\gamma(t)$ are given by

$$\hat{\boldsymbol{g}}_s(t) = \cos(\gamma(t) - \gamma_0)\,\hat{\boldsymbol{g}}_s(t_0) + \sin(\gamma(t) - \gamma_0)\,\hat{\boldsymbol{g}}_t(t_0) \tag{1}$$

$$\hat{\boldsymbol{g}}_t(t) = -\sin(\gamma(t) - \gamma_0)\,\hat{\boldsymbol{g}}_s(t_0) + \cos(\gamma(t) - \gamma_0)\,\hat{\boldsymbol{g}}_t(t_0) \tag{2}$$

The spin rate of the VSCMG about $\hat{\boldsymbol{g}}_s$ is denoted by Ω. The angular velocity vector of the $\mathcal{G}$ frame relative to the $\mathcal{B}$ frame is

$$\boldsymbol{\omega}_{\mathcal{G}/\mathcal{B}} = \dot{\gamma}\hat{\boldsymbol{g}}_g \tag{3}$$

The angular velocity vector of the reaction wheel frame $\mathcal{W}$ relative to the gimbal frame $\mathcal{G}$ is

$$\boldsymbol{\omega}_{\mathcal{W}/\mathcal{G}} = \Omega\hat{\boldsymbol{g}}_s \tag{4}$$

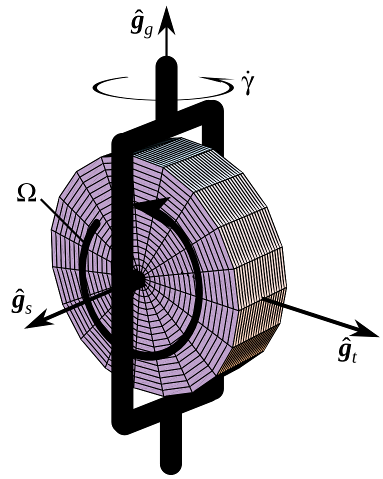

Figure 1: Illustration of a Variable Speed Control Moment Gyroscope

To indicate in which reference frame vector or matrix components are taken, a superscript letter is added before the vector or matrix name. Because the $\mathcal{G}$ frame unit axes are aligned with the principal gimbal frame axes, the gimbal frame inertia matrix $[I_G]$ expressed in the $\mathcal{G}$ frame is the constant diagonal matrix.

$$[I_G] = {}^{\mathcal{G}}[I_G] = \text{diag}(I_{G_s}, I_{G_t}, I_{G_g}) \tag{5}$$

where I_{G_s}, I_{G_t} and I_{G_g} are the gimbal frame inertias about the corresponding spin, transverse and gimbal axes. The reaction wheel inertia about the same axes are denoted by I_{W_s}, I_{W_t} and I_{W_t}.

$$[I_W] = {}^{\mathcal{W}}[I_W] = \text{diag}(I_{W_s}, I_{W_t}, I_{W_t}) \tag{6}$$

Note that since the disk is symmetric about the $\hat{\boldsymbol{g}}_s$ axis ${}^{\mathcal{W}}[I_W] = {}^{\mathcal{G}}[I_W]$. In practice I_{W_s} is typically much larger than any of the other gimbal frame or RW inertias. In this development the RW and gimbal frame inertias are not combined early on into one overall VSCMG inertia matrix; rather, they are retained as separate entities until later into the development. This will allow for a precise formulation of the actual physical motor torques that drive the RWs or the CMGs.

The $\mathcal{G}$ frame orientation is related to the $\mathcal{B}$ frame orientation through the direction cosine matrix $[BG]$ which is expressed in terms of the gimbal frame unit direction vectors as

$$[BG] = [\hat{\boldsymbol{g}}_s \, \hat{\boldsymbol{g}}_t \, \hat{\boldsymbol{g}}_g] \tag{7}$$

In Eq. (7) the $\hat{\boldsymbol{g}}_i$ vector components are taken in the $\mathcal{B}$ frame. The rotation matrix $[BG]$ maps a vector with components taken in the $\mathcal{G}$ frame into a vector with components in the $\mathcal{B}$ frame. The constant diagonal inertia matrices ${}^{\mathcal{G}}[I_G]$ and ${}^{\mathcal{G}}[I_W]$ are expressed with components taken in the $\mathcal{B}$ frame as the time varying matrices[8,9]

$${}^{\mathcal{B}}[I_G] = [BG]\,{}^{\mathcal{G}}[I_G]\,[BG]^T = I_{G_s}\hat{\boldsymbol{g}}_s\hat{\boldsymbol{g}}_s^T + I_{G_t}\hat{\boldsymbol{g}}_t\hat{\boldsymbol{g}}_t^T + I_{G_g}\hat{\boldsymbol{g}}_g\hat{\boldsymbol{g}}_g^T \tag{8}$$

$${}^{\mathcal{B}}[I_W] = [BG]\,{}^{\mathcal{G}}[I_W]\,[BG]^T = I_{W_s}\hat{\boldsymbol{g}}_s\hat{\boldsymbol{g}}_s^T + I_{W_t}\hat{\boldsymbol{g}}_t\hat{\boldsymbol{g}}_t^T + I_{W_t}\hat{\boldsymbol{g}}_g\hat{\boldsymbol{g}}_g^T \tag{9}$$

The total angular momentum of the spacecraft and the VSCMG about the spacecraft center of mass is given by

$$\boldsymbol{H} = \boldsymbol{H}_B + \boldsymbol{H}_G + \boldsymbol{H}_W \tag{10}$$

where $\boldsymbol{H}_B$ is the angular momentum component of the spacecraft, $\boldsymbol{H}_G$ is the angular momentum of the gimbal frame and $\boldsymbol{H}_W$ is the angular momentum of the RW. Let $\mathcal{N}$ be an inertial reference frame and $\boldsymbol{\omega}_{\mathcal{B}/\mathcal{N}}$ be the relative angular velocity vector, then $\boldsymbol{H}_B$ is written as

$$\boldsymbol{H}_B = [I_s]\boldsymbol{\omega}_{\mathcal{B}/\mathcal{N}} \tag{11}$$

The matrix $[I_s]$ contains the spacecraft inertias and the VSCMG inertia components due to the fact that the VSCMG center of mass is not located at the spacecraft center of mass. Note that ${}^{\mathcal{B}}[I_s]$ is a constant matrix as seen from the $\mathcal{B}$ frame. The gimbal frame angular momentum $\boldsymbol{H}_G$ is given by

$$\boldsymbol{H}_G = [I_G]\boldsymbol{\omega}_{\mathcal{G}/\mathcal{N}} \tag{12}$$

where $\boldsymbol{\omega}_{\mathcal{G}/\mathcal{N}} = \boldsymbol{\omega}_{\mathcal{G}/\mathcal{B}} + \boldsymbol{\omega}_{\mathcal{B}/\mathcal{N}}$. Using Eqs. (3), (5) and (8) this is rewritten as

$$\boldsymbol{H}_G = \left(I_{G_s}\hat{\boldsymbol{g}}_s\hat{\boldsymbol{g}}_s^T + I_{G_t}\hat{\boldsymbol{g}}_t\hat{\boldsymbol{g}}_t^T + I_{G_g}\hat{\boldsymbol{g}}_g\hat{\boldsymbol{g}}_g^T \right)\boldsymbol{\omega}_{\mathcal{B}/\mathcal{N}} + I_{G_g}\dot{\gamma}\hat{\boldsymbol{g}}_g \tag{13}$$

To simplify the following notation, let the variables ω_s, ω_t and ω_g be the projection of $\boldsymbol{\omega}_{\mathcal{B}/\mathcal{N}}$ onto the $\mathcal{G}$ frame unit axes.

$$\omega_s = \hat{\boldsymbol{g}}_s^T\boldsymbol{\omega}_{\mathcal{B}/\mathcal{N}} \qquad \omega_t = \hat{\boldsymbol{g}}_t^T\boldsymbol{\omega}_{\mathcal{B}/\mathcal{N}} \qquad \omega_g = \hat{\boldsymbol{g}}_g^T\boldsymbol{\omega}_{\mathcal{B}/\mathcal{N}} \tag{14}$$

The angular momentum $\boldsymbol{H}_G$ is then written as

$$\boldsymbol{H}_G = I_{G_s}\omega_s\hat{\boldsymbol{g}}_s + I_{G_t}\omega_t\hat{\boldsymbol{g}}_t + I_{G_g}\left(\omega_g + \dot{\gamma}\right)\hat{\boldsymbol{g}}_g \tag{15}$$

The RW angular momentum $\boldsymbol{H}_W$ is given by

$$\boldsymbol{H}_W = [I_W]\boldsymbol{\omega}_{\mathcal{W}/\mathcal{N}} \tag{16}$$

where $\boldsymbol{\omega}_{\mathcal{W}/\mathcal{N}} = \boldsymbol{\omega}_{\mathcal{W}/\mathcal{G}} + \boldsymbol{\omega}_{\mathcal{G}/\mathcal{B}} + \boldsymbol{\omega}_{\mathcal{B}/\mathcal{N}}$. Using analogous definitions as for $\boldsymbol{H}_G$, $\boldsymbol{H}_W$ is rewritten as

$$\boldsymbol{H}_W = I_{W_s}\left(\omega_s + \Omega\right)\hat{\boldsymbol{g}}_s + I_{W_t}\omega_t\hat{\boldsymbol{g}}_t + I_{W_t}\left(\omega_g + \dot{\gamma}\right)\hat{\boldsymbol{g}}_g \tag{17}$$

To simplify the notation from here on, let us use the short hand notation $\boldsymbol{\omega} = \boldsymbol{\omega}_{\mathcal{B}/\mathcal{N}}$. In some calculations it will be convenient to express $\boldsymbol{\omega}$ in the $\mathcal{G}$ frame as

$${}^{\mathcal{G}}\boldsymbol{\omega} = \omega_s\hat{\boldsymbol{g}}_s + \omega_t\hat{\boldsymbol{g}}_t + \omega_g\hat{\boldsymbol{g}}_g \tag{18}$$

To denote that a vector $\boldsymbol{x}$ is being differentiated relative to a reference frame $\mathcal{A}$, the following notation is used.

$$\frac{{}^{\mathcal{A}}d}{dt}\left(\boldsymbol{x}\right)$$

Indicating an inertial time derivatives of a vector $\boldsymbol{x}$ will be abbreviated as

$$\frac{{}^{\mathcal{N}}d}{dt}\left(\boldsymbol{x}\right) \equiv \dot{\boldsymbol{x}}$$

The equations of motion of a system of rigid bodies follow from Euler's equation[8, 9]

$$\dot{\boldsymbol{H}} = \boldsymbol{L} \tag{19}$$

if all moments are taken about the center of mass. The vector $\boldsymbol{L}$ represents the sum of all the external torques experienced by the spacecraft. The time derivative of $\boldsymbol{H}_W$ is expressed as expressed as

$$\begin{aligned}
\dot{\boldsymbol{H}}_W = {}& \hat{\boldsymbol{g}}_s I_{W_s}\left(\dot{\Omega} + \hat{\boldsymbol{g}}_s^T\dot{\boldsymbol{\omega}} + \dot{\gamma}\omega_t\right) \\
& + \hat{\boldsymbol{g}}_t\left(I_{W_s}\dot{\gamma}\omega_s + I_{W_t}\hat{\boldsymbol{g}}_t^T\dot{\boldsymbol{\omega}} + \left(I_{W_s} - I_{W_t}\right)\omega_s\omega_g + I_{W_s}\Omega\left(\dot{\gamma} + \omega_g\right)\right) \\
& + \hat{\boldsymbol{g}}_g\left(I_{W_t}\hat{\boldsymbol{g}}_g^T\left(\dot{\boldsymbol{\omega}} + \ddot{\gamma}\right) + \left(I_{W_t} - I_{W_s}\right)\omega_s\omega_t + I_{W_s}\Omega\omega_t\right)
\end{aligned} \tag{20}$$

Let $\boldsymbol{L}_W$ be the torque the gimbal frame exerts on the RW. Euler's equation for the RW is $\dot{\boldsymbol{H}}_W = \boldsymbol{L}_W$. The torque components in the $\hat{\boldsymbol{g}}_t$ and $\hat{\boldsymbol{g}}_g$ direction are produced by the gimbal frame itself. However, the torque component u_s about the $\hat{\boldsymbol{g}}_s$ axis is produced by the RW torque motor. Therefore, from Eq. (20) the spin control torque u_s is given by

$$u_s = I_{W_s}\left(\dot{\Omega} + \hat{\boldsymbol{g}}_s^T\dot{\boldsymbol{\omega}} + \dot{\gamma}\omega_t\right) \tag{21}$$

Differentiating Eq. (15), the momentum rate $\dot{\boldsymbol{H}}_G$ is written as

$$\begin{aligned}\dot{\boldsymbol{H}}_G = \hat{\boldsymbol{g}}_s &\left(\left(I_{G_s} - I_{G_t} + I_{G_g}\right)\dot{\gamma}\omega_t + I_{G_s}\hat{\boldsymbol{g}}_s^T\dot{\boldsymbol{\omega}} + \left(I_{G_g} - I_{G_t}\right)\omega_t\omega_g\right)\\ &+ \hat{\boldsymbol{g}}_t\left(\left(I_{G_s} - I_{G_t} - I_{G_g}\right)\dot{\gamma}\omega_s + I_{G_t}\hat{\boldsymbol{g}}_t^T\dot{\boldsymbol{\omega}} + \left(I_{G_s} - I_{G_t}\right)\omega_s\omega_g\right)\\ &+ \hat{\boldsymbol{g}}_g\left(I_{G_g}\left(\hat{\boldsymbol{g}}_g^T\dot{\boldsymbol{\omega}} + \ddot{\gamma}\right) + \left(I_{G_t} - I_{G_s}\right)\omega_s\omega_t\right)\end{aligned} \tag{22}$$

From here on it is convenient to combine the inertia matrices of the RW and the gimbal frame into one VSCMG inertia matrix $[J]$ as

$$[J] = [I_G] + [I_W] = \text{diag}(J_s, J_t, J_g) \tag{23}$$

Let $\boldsymbol{L}_G$ be the torque vector that the combined RW and CMG system exerts onto the spacecraft, then Euler's equation states that $\dot{\boldsymbol{H}}_G + \dot{\boldsymbol{H}}_W = \boldsymbol{L}_G$. The $\boldsymbol{L}_G$ torque component about the $\hat{\boldsymbol{g}}_g$ axis is produced by the gimbal torque motor. Adding Eqs. (20) and (22) and making use of the definition in Eq. (23), the gimbal torque u_g is then expressed as

$$u_g = J_g\left(\hat{\boldsymbol{g}}_g^T\dot{\boldsymbol{\omega}} + \ddot{\gamma}\right) - \left(J_s - J_t\right)\omega_s\omega_t - I_{W_s}\Omega\omega_t \tag{24}$$

The inertial derivative of $\boldsymbol{H}_B$ is simply

$$\dot{\boldsymbol{H}}_B = [I_s]\dot{\boldsymbol{\omega}} + [\tilde{\boldsymbol{\omega}}][I_s]\boldsymbol{\omega} \tag{25}$$

where the tilde matrix operator $[\tilde{\boldsymbol{\omega}}]$ is defined as

$$[\tilde{\boldsymbol{\omega}}] = \begin{bmatrix} 0 & -\omega_3 & \omega_2 \\ \omega_3 & 0 & -\omega_1 \\ -\omega_2 & \omega_1 & 0 \end{bmatrix} \tag{26}$$

To further simplify the equations of motions, we define the total spacecraft inertia matrix $[I]$ as

$$[I] = [I_s] + [J] \tag{27}$$

Substituting Eqs. (20), (22) and (25) back into Eq. (19) and making use of the definition in Eq. (27), we find the equations of motion for a rigid spacecraft containing one VSCMG.

$$\begin{aligned}[I]\dot{\boldsymbol{\omega}} = -[\tilde{\boldsymbol{\omega}}][I]\boldsymbol{\omega} &- \hat{\boldsymbol{g}}_s\left(J_s\dot{\gamma}\omega_t + I_{W_s}\dot{\Omega} - \left(J_t - J_g\right)\omega_t\dot{\gamma}\right)\\ &- \hat{\boldsymbol{g}}_t\left(\left(J_s\omega_s + I_{W_s}\Omega\right)\dot{\gamma} - \left(J_t + J_g\right)\omega_s\dot{\gamma} + I_{W_s}\Omega\omega_g\right)\\ &- \hat{\boldsymbol{g}}_g\left(J_g\ddot{\gamma} - I_{W_s}\Omega\omega_t\right) + \boldsymbol{L}\end{aligned} \tag{28}$$

At this point, we make the common assumption that $J_s \approx I_{W_s}$, i.e,. that the gimbal frame inertia I_{G_s} about the spin axis is negligible. The corresponding equations of motion are simplified to

$$\begin{aligned}[I]\dot{\boldsymbol{\omega}} = -[\tilde{\boldsymbol{\omega}}][I]\boldsymbol{\omega} &- \hat{\boldsymbol{g}}_s\left(J_s\left(\dot{\Omega} + \dot{\gamma}\omega_t\right) - \left(J_t - J_g\right)\omega_t\dot{\gamma}\right)\\ &- \hat{\boldsymbol{g}}_t\left(J_s\left(\omega_s + \Omega\right)\dot{\gamma} - \left(J_t + J_g\right)\omega_s\dot{\gamma} + J_s\Omega\omega_g\right)\\ &- \hat{\boldsymbol{g}}_g\left(J_g\ddot{\gamma} - J_s\Omega\omega_t\right) + \boldsymbol{L}\end{aligned} \tag{29}$$

To obtain the equations of motion of a rigid spacecraft with several VSCMGs attached, we add the effects of each $\dot{\boldsymbol{H}}_G$ and $\dot{\boldsymbol{H}}_W$. To simplify notation, let us define the following useful matrices. The matrices $[G_s]$, $[G_t]$ and $[G_g]$ contain the unit direction vectors of each VSCMG gimbal frame.

$$[G_s] = [\hat{\boldsymbol{g}}_{s_1} \cdots \hat{\boldsymbol{g}}_{s_N}] \qquad [G_t] = [\hat{\boldsymbol{g}}_{t_1} \cdots \hat{\boldsymbol{g}}_{t_N}] \qquad [G_g] = [\hat{\boldsymbol{g}}_{g_1} \cdots \hat{\boldsymbol{g}}_{g_N}] \tag{30}$$

The total spacecraft inertia matrix is expressed as

$$[I] = [I_s] + \sum_{i=1}^{N} [J_i] = [I_s] + \sum_{i=1}^{N} J_{s_i} \hat{\boldsymbol{g}}_{s_i} \hat{\boldsymbol{g}}_{s_i}^T + J_{t_i} \hat{\boldsymbol{g}}_{t_i} \hat{\boldsymbol{g}}_{t_i}^T + J_{g_i} \hat{\boldsymbol{g}}_{g_i} \hat{\boldsymbol{g}}_{g_i}^T \tag{31}$$

The effective torque quantities τ_{s_i}, τ_{t_i} and τ_{g_i} are defined as

$$\boldsymbol{\tau}_s = \begin{bmatrix} J_{s_1}\left(\dot{\Omega}_1 + \dot{\gamma}_1 \omega_{t_1}\right) - \left(J_{t_1} - J_{g_1}\right)\omega_{t_1}\dot{\gamma}_1 \\ \vdots \\ J_{s_N}\left(\dot{\Omega}_N + \dot{\gamma}_N \omega_{t_N}\right) - \left(J_{t_N} - J_{g_N}\right)\omega_{t_N}\dot{\gamma}_N \end{bmatrix} \tag{32a}$$

$$\boldsymbol{\tau}_s = \begin{bmatrix} J_{s_1}\left(\Omega_1 + \omega_{s_1}\right)\dot{\gamma}_1 - \left(J_{t_1} + J_{g_1}\right)\omega_{s_1}\dot{\gamma}_1 + J_{s_1}\Omega_1\omega_{g_1} \\ \vdots \\ J_{s_N}\left(\Omega_N + \omega_{s_N}\right)\dot{\gamma}_N - \left(J_{t_N} + J_{g_N}\right)\omega_{s_N}\dot{\gamma}_N + J_{s_N}\Omega_N\omega_{g_N} \end{bmatrix} \tag{32b}$$

$$\boldsymbol{\tau}_g = \begin{bmatrix} J_{g_1}\ddot{\gamma}_1 - J_{s_1}\Omega_1\omega_{t_1} \\ \vdots \\ J_{g_N}\ddot{\gamma}_N - J_{s_N}\Omega_N\omega_{t_N} \end{bmatrix} \tag{32c}$$

The rotational equations of motion for a rigid body containing N VSCMGs are then written compactly as

$$[I]\dot{\boldsymbol{\omega}} = -[\tilde{\boldsymbol{\omega}}][I]\boldsymbol{\omega} - [G_s]\boldsymbol{\tau}_s - [G_t]\boldsymbol{\tau}_t - [G_g]\boldsymbol{\tau}_g + \boldsymbol{L} \tag{33}$$

Also, The rotational kinetic energy T of a rigid spacecraft with N VSCMGs is given by

$$T = \frac{1}{2}\boldsymbol{\omega}^T[I_s]\boldsymbol{\omega} + \frac{1}{2}\sum_{i=1}^{N} J_{s_i}\left(\Omega_i + \omega_{s_i}\right)^2 + J_{t_i}\omega_{t_i}^2 + J_{g_i}\left(\omega_{g_i} + \dot{\gamma}_i\right)^2 \tag{34}$$

The kinetic energy or work rate, found after differentiating Eq. (34) with respect to time and performing some lengthy algebra, is found to be

$$\dot{T} = \sum_{i=1}^{N} \dot{\gamma}_i u_{g_i} + \Omega_i u_{s_i} + \boldsymbol{\omega}^T \boldsymbol{L} \tag{35}$$

Actually, the energy rate expression for this system of rigid bodies was known apriori from the Work-Energy-Rate principle.[10] Hence, the derivation of Eq. (35) from the equations of motion validates the equations of motion.

Feedback Control Law

In this section, a feedback law is derived using Lyapunov control theory. Given some initial angular velocity and attitude measure, the goal of the control law is to bring the rigid body to rest at the zero attitude (aligned with the reference frame). The attitude coordinate system is chosen such that the zero attitude is the desired attitude. To describe the rigid spacecraft attitude, this paper uses the very elegant set of recently developed Modified Rodrigues Parameters (MRP) along with their "shadow" counterparts.[11,12,13,14,15,16] They allow for a non-singular rigid body attitude description with several other useful attributes. The MRPs can be defined in terms of the Euler parameters $\boldsymbol{\beta}$ as[11,13,16]

$$\sigma_i = \frac{\beta_i}{1+\beta_0} \qquad i = 1,2,3 \tag{36}$$

Or, in terms of the principal rotation axis $\hat{e}$ and the principal rotating angle ϕ, the MRP vector is

$$\boldsymbol{\sigma} = \hat{\boldsymbol{e}} \cdot \tan(\phi/4) \tag{37}$$

Note that the tangent function typically behaves very linearly for angles up to 20 degrees. Since Eq. (37) shows that $\boldsymbol{\sigma}$ is written in terms of $\tan(\phi/4)$, the MRPs behave very linearly for principal rotations up to ± 80 degrees. This is a much larger range of rotations that can be assumed to behave near-linearly than what can be typically achieved using standard Euler Angles or even the classical Rodrigues parameters.

Like the Euler parameters, the modified Rodrigues parameters are not unique. A second set of modified Rodrigues parameters, called the "shadow" set, can be used to avoid the singularity of the "original" MRP at $\phi = \pm 360°$ at the cost of a discontinuity at a switching point. The transformation between the "original" and "shadow" sets of MRPs for any arbitrary switching surface $\boldsymbol{\sigma}^T\boldsymbol{\sigma} =$ constant is[11,17,15]

$$\boldsymbol{\sigma}^S = -\frac{\boldsymbol{\sigma}}{\boldsymbol{\sigma}^T\boldsymbol{\sigma}} \tag{38}$$

Typically the MRP vector $\boldsymbol{\sigma}$ is switched to it's alternate set whenever $\boldsymbol{\sigma}^T\boldsymbol{\sigma} > 1$ which corresponds to the rigid body having tumbled past $\phi = \pm 180$ degrees. The MRP differential kinematic equation only contains a quadratic nonlinearity and is given by

$$\frac{d\boldsymbol{\sigma}}{dt} = \frac{1}{2}\left[[I_{3\times3}]\left(\frac{1-\boldsymbol{\sigma}^T\boldsymbol{\sigma}}{2}\right) + [\tilde{\boldsymbol{\sigma}}] + \boldsymbol{\sigma}\boldsymbol{\sigma}^T\right]\boldsymbol{\omega}_{\mathcal{B}/\mathcal{N}} \tag{39}$$

where $[I_{3x3}]$ is a 3x3 identity matrix. In designing the control law, we assume that estimates of $\boldsymbol{\omega}$, $\boldsymbol{\sigma}$, Ω_i and γ_i are available. The following Lyapunov function V is a positive definite, radially unbounded measure of the total system state error relative to the target state $\boldsymbol{\omega} = \boldsymbol{\sigma} = 0$ where K is a scalar attitude feedback gain.[6]

$$V(\boldsymbol{\omega},\boldsymbol{\sigma}) = \frac{1}{2}\boldsymbol{\omega}^T[I]\boldsymbol{\omega} + 2K\log\left(1+\boldsymbol{\sigma}^T\boldsymbol{\sigma}\right) \tag{40}$$

The use of the logarithm function in this context was first introduced by Tsiotras in Ref. 13 and leads to a control law which is linear in σ. Using Eqs. (14) and (31) the Lyapunov function is rewritten as

$$V = \frac{1}{2}\boldsymbol{\omega}^T[I_s]\boldsymbol{\omega} + \frac{1}{2}\sum_{i=1}^{N}\left(J_{s_i}\omega_{s_i}^2 + J_{t_i}\omega_{t_i}^2 + J_{g_i}\omega_{g_i}^2\right) + 2K\log\left(1+\boldsymbol{\sigma}^T\boldsymbol{\sigma}\right) \tag{41}$$

Differentiating the Lyapunov function V yields

$$\dot{V} = \boldsymbol{\omega}^T\left([I]\dot{\boldsymbol{\omega}} + \sum_{i=1}^{N}\left(J_{s_i} - J_{t_i}\right)\dot{\gamma}_i\omega_{t_i}\hat{\boldsymbol{g}}_{s_i} + K\boldsymbol{\sigma}\right) \tag{42}$$

Lyapunov stability theory requires that $\dot{V}$ be negative semi-definite to guarantee stability. Let $[P]$ be a positive definite angular velocity feedback gain matrix, then $\dot{V}$ is set to be

$$\dot{V} = -\boldsymbol{\omega}^T[P]\boldsymbol{\omega} \tag{43}$$

which, when combined with Eq. (42), leads to the following condition for stability.

$$[I]\dot{\boldsymbol{\omega}} = -K\boldsymbol{\sigma} - [P]\boldsymbol{\omega} - \sum_{i=1}^{N} \left(J_{s_i} - J_{t_i}\right) \dot{\gamma}_i \omega_{t_i} \hat{\boldsymbol{g}}_{s_i} \tag{44}$$

After substituting the equations of motion given in Eq. (33) into Eq. (44) and simplifying the result, the following stability requirement is obtained.

$$\sum_{i=1}^{N} \left(\hat{\boldsymbol{g}}_{s_i} J_{s_i} \dot{\Omega}_i + \hat{\boldsymbol{g}}_{g_i} J_{g_i} \ddot{\gamma}_i + \hat{\boldsymbol{g}}_{t_i} \left(J_{s_i} \left(\Omega_i + \omega_{s_i}\right) - J_{t_i} \omega_{s_i}\right) \dot{\gamma}_i \right) = K\boldsymbol{\sigma} + [P]\boldsymbol{\omega} + \boldsymbol{L} \tag{45}$$

To express this condition in a more compact and useable form, let us define the following *3*xN matrices.

$$[D_0] = [\hat{\boldsymbol{g}}_{s_1} J_{s_1} \cdots \hat{\boldsymbol{g}}_{s_N} J_{s_N}] \tag{46a}$$
$$[D_1] = [\hat{\boldsymbol{g}}_{t_1} J_{s_1} \left(\Omega_1 + \omega_{s_1}\right) \cdots \hat{\boldsymbol{g}}_{t_N} J_{s_N} \left(\Omega_N + \omega_{s_N}\right)] \tag{46b}$$
$$[D_2] = [\hat{\boldsymbol{g}}_{t_1} J_{t_1} \omega_{s_1} \cdots \hat{\boldsymbol{g}}_{t_N} J_{t_N} \omega_{s_N}] \tag{46c}$$
$$[B] = [\hat{\boldsymbol{g}}_{g_1} J_{g_1} \cdots \hat{\boldsymbol{g}}_{g_N} J_{g_N}] \tag{46d}$$

Let $\dot{\boldsymbol{\Omega}}$, $\ddot{\boldsymbol{\gamma}}$ and $\dot{\boldsymbol{\gamma}}$ be Nx*1* vectors whose *i*-th element contains the respective VSCMG angular velocity or acceleration or RW spin rate. Then the stability condition in Eq. (45) is

$$[D_0]\dot{\boldsymbol{\Omega}} + [B]\ddot{\boldsymbol{\gamma}} + \left([D_1] - [D_2]\right)\dot{\boldsymbol{\gamma}} = \boldsymbol{L}_r \tag{47}$$

where $\boldsymbol{L}_r = K\boldsymbol{\sigma} + [P]\boldsymbol{\omega} + \boldsymbol{L}$ is called the required control torque. Dropping the $[D_0]\dot{\boldsymbol{\Omega}}$ term, the standard single-gimbal CMG stability condition is retrieved as it is developed in Ref. 1. Note that the condition in Eq. (47) only guarantees global stability in the sense of Lyapunov for the states $\boldsymbol{\omega}$ and $\boldsymbol{\sigma}$ because $\dot{V}$ in Eq. (43) is only negative semi-definite, not negative definite. However, Eq. (43) does show that $\boldsymbol{\omega} \to 0$ as time goes to infinity. To prove that the stability condition in Eq. (47) guarantees asymptotic stability of all states including $\boldsymbol{\sigma}$, the higher order time derivatives of V must be investigated. A sufficient condition to guarantee asymptotic stability is that the first nonzero higher-order derivative of V, evaluated on the set of states such that $\dot{V}$ is zero, must be of odd order and be negative definite.[18,19,20] For this dynamical system $\dot{V}$ is zero when $\boldsymbol{\omega}$ is zero. Differentiating Eq. (43), the second derivative of V is

$$\frac{d^2}{dt^2}V = -2\boldsymbol{\omega}^T[P]\dot{\boldsymbol{\omega}} \tag{48}$$

which is zero on the set of states where $\boldsymbol{\omega}$ is zero. Differentiating again, the third derivative of V is

$$\frac{d^3}{dt^3}V = -2\dot{\boldsymbol{\omega}}^T[P]\dot{\boldsymbol{\omega}} - 2\boldsymbol{\omega}^T[P]\ddot{\boldsymbol{\omega}} \tag{49}$$

By substituting Eq. (44) and setting $\boldsymbol{\omega} = 0$, we may express the third derivative of the Lyapunov function as

$$\frac{d^3}{dt^3}V = -K^2\boldsymbol{\sigma}^T \left([I]^{-1}\right)^T [P][I]^{-1}\boldsymbol{\sigma} \tag{50}$$

which is a negative definite quantity because both $[I]$ and $[P]$ are positive definite matrices. Therefore the stability condition in Eq. (47) does guarantee global asymptotic stability.

Velocity Based Steering Law

Note that the stability condition in Eq. (47) does not contain the physical control torques u_{s_i} and u_{g_i} explicitly. Instead only gimbal rates and accelerations and RW accelerations appear. This will lead to a steering law that determines the required time history of $\boldsymbol{\gamma}$ and $\boldsymbol{\Omega}$ such that Eq. (47) is satisfied. The reason for this is two fold. First, commercial CMGs typically require $\dot{\boldsymbol{\gamma}}$ as the input, not the actual physical torque vector $\boldsymbol{u}_g$. Secondly, writing Eq. (47) in terms of the torque vectors $\boldsymbol{u}_s$ and $\boldsymbol{u}_g$ and then solving for these would lead to a control law that is equivalent to solving Eq. (47) directly for $\ddot{\boldsymbol{\gamma}}$. As has been pointed out in Ref. 1, this leads to a very undesirable control law with excessive gimbal rates. A physical reason for this is that such control laws provide the required control torque mainly through the $[B]\ddot{\boldsymbol{\gamma}}$ term. In this setup the CMGs are essentially being used as RWs and the potential torque amplification effect in not being exploited. Because CMG gimbal inertias J_g are typically very small compared to their spin inertia J_s, the corresponding $[B]$ will also be very small which leads to very large $\ddot{\boldsymbol{\gamma}}$ vectors.

To take advantage of the potential torque amplification effect, most of the required control torque vector $\boldsymbol{L}_r$ should be produced by the $([D_1] - [D_2])\,\dot{\boldsymbol{\gamma}}$ term. This is why classical CMG steering laws control primarily the $\dot{\boldsymbol{\gamma}}$ vector and not $\ddot{\boldsymbol{\gamma}}$. For the VSCMGs it is desirable to have the required torque $\boldsymbol{L}_r$ be produced by a combination of the $\dot{\boldsymbol{\Omega}}$ and $\dot{\boldsymbol{\gamma}}$ terms in Eq. (47). Paralleling the development of the classical single-gimbal CMG velocity steering laws, the terms containing the transverse and gimbal VSCMG inertias are ignored at this level. Eq. (47) then becomes

$$[D_0]\dot{\boldsymbol{\Omega}} + [D_1]\dot{\boldsymbol{\gamma}} = \boldsymbol{L}_r \tag{51}$$

Comparing the $[D_1]$ matrix to that of standard CMG steering laws it is evident that an extra $\hat{\boldsymbol{g}}_t J_s \omega_s$ term is present in the VSCMG formulation. This term is also dropped in the standard CMG formulation because it can be assumed that ω_s will typically be much smaller than Ω. However, since for a VSCMG the RW spin speed Ω is variable, this assumption can no longer be justified and this term is retained in this formulation.

For notational convenience, we introduce the *2N*x*1* state vector $\boldsymbol{\eta}$

$$\boldsymbol{\eta} = \begin{bmatrix} \boldsymbol{\Omega} \\ \gamma \end{bmatrix} \tag{52}$$

and the *3*x*2N* matrix $[Q]$

$$[Q] = \left[D_0 \,\vdots\, D_1 \right] \tag{53}$$

Eq. (51) can then be written compactly as

$$[Q]\dot{\boldsymbol{\eta}} = \boldsymbol{L}_r \tag{54}$$

Note that each column of the $[D_0]$ matrix is a scalar multiple of the $\hat{\boldsymbol{g}}_{s_i}$ vectors, while each column of $[D_1]$ is a scalar multiple of the $\hat{\boldsymbol{g}}_{t_i}$ vectors. In the classical 4 single-gimbal CMG cluster, singular gimbal configurations are encountered whenever the rank of $[D_1]$ is less than 3. This occurs whenever the $\hat{\boldsymbol{g}}_{t_i}$ no longer span the three-dimensional space but form a plane. If this occurs, any required torque which does not lie perfectly in this plane is not generated exactly by the CMG cluster and the spacecraft deviates slightly from the desired attitude. If the required control torque is perpendicular to this plane, then the CMG cluster produces no effective torque on the spacecraft. These singular configurations can never occur with a VSCMG because the rank of the $[Q]$ matrix will never be less than 3! Since the $\hat{\boldsymbol{g}}_{s_i}$ vectors are perpendicular to the $\hat{\boldsymbol{g}}_{t_i}$ vectors, even when all the transverse axes are coplanar, there will always be at least one spin axis that is not in this plane. Therefore the columns of $[Q]$ will *always* span the entire three-dimensional space as long as at least 2 or more VSCMGs are used with unique $\hat{\boldsymbol{g}}_{g_i}$ vectors.

Because the $[Q]$ matrix is never rank deficient, a minimum norm solution for $\dot{\boldsymbol{\eta}}$ can be obtained using the standard Moore-Penrose inverse. However, because ideally the VSCMGs are to act like classical CMGs away from single-gimbal CMG singular configurations, a weighted pseudo inverse is used instead.[21] Let $[W]$ be a $2N$x$2N$ diagonal matrix

$$[W] = diag\{W_{s_1}, \dots, W_{s_N}, W_{g_1}, \dots, W_{g_N}\} \tag{55}$$

where W_{s_i} and W_{g_i} are the weights associated with how nearly the VSCMGs are to perform like regular RWs or CMGs. Then, the desired $\dot{\boldsymbol{\eta}}$ is

$$\dot{\boldsymbol{\eta}} = \begin{bmatrix} \dot{\boldsymbol{\Omega}} \\ \dot{\boldsymbol{\gamma}} \end{bmatrix} = [W][Q]^T \left([Q][W][Q]^T\right)^{-1} \boldsymbol{L}_r \tag{56}$$

Note that there is no need here to introduce a modified pseudo-inverse as Nakamura and Hanafusa did in developing the singularity robustness steering law in Ref. 22. To achieve the desired VSCMG behavior, the weights are made dependent on the proximity to a single-gimbal CMG singularity. To measure this proximity the scalar factor δ is defined as

$$\delta = \det\left([D_1][D_1]^T\right) \tag{57}$$

As the gimbal angles approach a singular CMG configuration this parameter δ will go to zero. The weights W_{s_i} are then defined to be

$$W_{s_i} = W_{s_i}^0 e^{(-\mu\delta)} \tag{58}$$

where $W_{s_i}^0$ and μ are positive scalars to be chosen by the control designer. The gains W_{g_i} are simply held constant. Away from CMG singularities this steering law will have very small weights on the RW mode and essentially perform like a classical single-gimbal CMG. As a singularity is approached, the steering law will start to use the RW mode to ensure that the gimbal rates do not become excessive and that the required control torque $\boldsymbol{L}_r$ is actually produced by the VSCMG cluster.

Two types of CMG singularities are commonly discussed. The simpler type of singularity is when the rank of the $[D_1]$ matrix drops below 3 which is indicated by δ, defined in Eq. (57), approaching or becoming zero. The VSCMG velocity steering law in Eq. (56) handles temporary rank deficiencies very well. The required control torque is always produced correctly by making use of the addition control authority provided by the RW modes. Another type of singularity is when the required control torque is exactly perpendicular to the span of the transverse VSCMG axis (i.e. $\boldsymbol{L}_r$ is in the nullspace of $[D_1]$). Naturally, this is only possible whenever δ is zero. To measure how close the required torque $\boldsymbol{L}_r$ is to the nullspace of $[D_1]$ the orthogonality index $\mathcal{O}$ is used.[1]

$$\mathcal{O} = \frac{\boldsymbol{L}_r^T [D_1]^T [D_1] \boldsymbol{L}_r}{||\boldsymbol{L}_r||^2} \tag{59}$$

Whenever $\boldsymbol{L}_r$ becomes part of the nullspace of $[D_1]$, then $\mathcal{O}$ will tend towards zero. A classical single-gimbal CMG steering law demands a zero $\dot{\boldsymbol{\gamma}}$ vector with this type of singularity which "locks up" the gimbals produces no effective torque on the spacecraft. The VSCMG steering does not prevent the gimbals from being locked up in these singular orientations; however, the $\boldsymbol{L}_r$ vector is still being produced thanks to the RW mode of the VSCMGs. If a gimbal lock is actually achieved, then without any further changes, such as a change in the required $\boldsymbol{L}_r$, the VSCMG will simply continue the maneuvers acting like pure RWs. Running numerical simulations it was found that unless one starts the simulation in a pure gimbal lock situation, it was very unlikely for the VSCMG steering law to lock up the gimbals. Once a singularity is approached, the RWs are spun up or down which also in return affects the gimbal orientation and lowers the likelihood of having the orthogonality index $\mathcal{O}$ go to zero. However, at present this VSCMG steering law makes no explicit effort to avoid these singular configurations during a maneuver.

Acceleration Based Steering Law

The simplified formulation provided by the gimbal velocity based steering law in Eq. (56) is convenient to study and analyze the steering law. However, to provide a more realistic simulation, the transverse inertia should be included and $\ddot{\boldsymbol{\gamma}}$ should be used as the actual control input. Having a gimbal angle acceleration expression will also allow for simulations that study the actual work done by the steering laws. If the transverse inertias are considered, then the stability condition in Eq. (45) is given by

$$[D_0]\dot{\boldsymbol{\Omega}} + [B]\ddot{\boldsymbol{\gamma}} + [D]\dot{\boldsymbol{\gamma}} = \boldsymbol{L}_r \tag{60}$$

where $[D] = [D_1] + [D_2]$. The goal of the gimbal acceleration based steering law is to provide the same performance as the gimbal velocity based steering law. Let the vector $\dot{\boldsymbol{\eta}}_d$ be the desired $\dot{\boldsymbol{\Omega}}$ and $\dot{\boldsymbol{\gamma}}$ quantities provided by Eq. (56).

$$\dot{\boldsymbol{\eta}}_d = [W][Q]^T \left([Q][W][Q]^T\right)^{-1} \boldsymbol{L}_r \tag{61}$$

where the matrix $[Q]$ is now defined as

$$[Q] = \begin{bmatrix} D_0 \ \vdots \ D \end{bmatrix} \tag{62}$$

The vector $\dot{\boldsymbol{\eta}}$ contains the actual $\boldsymbol{\Omega}$ and $\dot{\boldsymbol{\gamma}}$ states. As is done with CMG steering laws in Ref. 1, a feedback law is designed around the desired $\dot{\boldsymbol{\eta}}_d$ such that the current $\boldsymbol{\eta}$ will approach $\dot{\boldsymbol{\eta}}_d$. To accomplish this we define the positive definite Lyapunov function $V_{\dot{\gamma}}$ as

$$V_{\dot{\gamma}} = \frac{1}{2}\left(\dot{\boldsymbol{\eta}}_d - \dot{\boldsymbol{\eta}}\right)^T \left(\dot{\boldsymbol{\eta}}_d - \dot{\boldsymbol{\eta}}\right) \tag{63}$$

with the derivative

$$\dot{V}_{\dot{\gamma}} = \left(\dot{\boldsymbol{\eta}}_d - \dot{\boldsymbol{\eta}}\right)^T \left(\ddot{\boldsymbol{\eta}}_d - \ddot{\boldsymbol{\eta}}\right) \tag{64}$$

To guarantee global asymptotic stability, $\dot{V}_{\dot{\gamma}}$ is set to

$$\dot{V}_{\dot{\gamma}} = -K_{\dot{\gamma}}\left(\dot{\boldsymbol{\eta}}_d - \dot{\boldsymbol{\eta}}\right)^T \left(\dot{\boldsymbol{\eta}}_d - \dot{\boldsymbol{\eta}}\right) \tag{65}$$

where $K_{\dot{\gamma}}$ is a positive scalar quantity. This leads to the following stability condition.

$$\ddot{\boldsymbol{\eta}} = K_{\dot{\gamma}}\left(\dot{\boldsymbol{\eta}}_d - \dot{\boldsymbol{\eta}}\right) + \ddot{\boldsymbol{\eta}}_d \tag{66}$$

As was done in designing the single-gimbal CMG acceleration steering law in Ref. 1, the vector $\ddot{\boldsymbol{\eta}}_d$ is assumed to be small and is neglected. Substituting Eq. (61) into (66) we get

$$\ddot{\boldsymbol{\eta}} = \begin{bmatrix} \ddot{\boldsymbol{\Omega}} \\ \ddot{\boldsymbol{\gamma}} \end{bmatrix} = K_{\dot{\gamma}}\left([W][Q]^T \left([Q][W][Q]^T\right)^{-1} \boldsymbol{L}_r - \begin{bmatrix} \dot{\boldsymbol{\Omega}} \\ \dot{\boldsymbol{\gamma}} \end{bmatrix}\right) \tag{67}$$

The vector $\ddot{\boldsymbol{\gamma}}$ is the desired gimbal angle acceleration vector. The vector $\ddot{\boldsymbol{\Omega}}$, which represents the reaction wheel "jerk", is also assumed to be very small and is neglected. After some algebraic manipulations, the desired RW and CMG angular acceleration vectors are given through the steering law

$$\begin{bmatrix} \dot{\boldsymbol{\Omega}} \\ \ddot{\boldsymbol{\gamma}} \end{bmatrix} = \begin{bmatrix} I & 0 \\ 0 & K_{\dot{\gamma}} I \end{bmatrix}\left([W][Q]^T \left([Q][W][Q]^T\right)^{-1} \boldsymbol{L}_r - \begin{bmatrix} 0 \\ \dot{\boldsymbol{\gamma}} \end{bmatrix}\right) \tag{68}$$

Note that the RW angular acceleration vector $\dot{\boldsymbol{\Omega}}$ in Eq. (68) is the same as is commanded by the velocity based steering law in Eq. (56). Since generally the initial $\dot{\boldsymbol{\gamma}}$ vector will not be equal to the desired velocity vector at the beginning of a maneuver, the gimbal acceleration vector $\ddot{\boldsymbol{\gamma}}$ will drive the gimbal velocities to the desired values and then remain relatively small.

Reconfiguring the VSCMG Cluster using Null Motion

To perform a given spacecraft maneuver, there are infinitely many CMG configurations that would produce the required torques. Depending on the torque direction and a given CMG momentum, some of these initial gimbal configurations will encounter CMG singularities during the resulting maneuver, while others will not. Vadali, et al. show in Ref. 23 a method for computing a preferred set of initial gimbal angles $\boldsymbol{\gamma}(t_0)$ for which the maneuver will not encounter any CMG singularities. To reorient the CMG cluster to these preferred gimbal angles without producing an effective torque onto the spacecraft, the null motion of $[D_1]\dot{\boldsymbol{\gamma}} = \boldsymbol{L}_r$ is used. However, the set of gimbal angles between which one can reorient the classical CMGs is very limited, because the inertial CMG cluster momentum vector must remain constant. Also, the null motion involves the inverse of the $[D_1][D_1]^T$ matrix which has to be approximated with the singularity robustness inverse whenever the determinant goes to zero. This approximation results in a small torque being applied to the spacecraft itself.

If the VSCMGs are rearranged, however, there are now twice as many degrees of control available. In particular, the CMG angles can be rearranged in a more general manner by also varying the RW spin speed vector $\boldsymbol{\Omega}$. The null motion of Eq. (54) is given by

$$\dot{\boldsymbol{\eta}} = \left[[I_{N\times N}] - [W][Q]^T\left([Q][W][Q]^T\right)^{-1}[Q]\right]\boldsymbol{d} = [\tau]\boldsymbol{d} \tag{69}$$

Note that the symmetric matrix $[\tau]$ is a projection matrix and has the useful property that $[\tau]^2 = [\tau]$. Let the constant vector $\boldsymbol{\eta}_f$ be the preferred set of $\boldsymbol{\Omega}_f$ and $\boldsymbol{\gamma}_f$. The error vector $\boldsymbol{e}$ is defined as

$$\boldsymbol{e} = [A]\left(\boldsymbol{\eta}_f - \boldsymbol{\eta}\right) \tag{70}$$

where $[A]$ is the diagonal matrix

$$[A] = \begin{bmatrix} a_{RW}[I_{N\times N}] & [0_{N\times N}] \\ [0_{N\times N}] & a_{CMG}[I_{N\times N}] \end{bmatrix} \tag{71}$$

The parameters a_{RW} and a_{CMG} are either 1 or 0. If one is set to zero, this means that the resulting null motion will be performed with no preferred set of either $\boldsymbol{\Omega}_f$ or $\boldsymbol{\gamma}_f$. The derivative of $\boldsymbol{e}$ is

$$\dot{\boldsymbol{e}} = -[A]\dot{\boldsymbol{\eta}} \tag{72}$$

The total error between preferred and actual states is given through the Lyapunov function

$$V_e(\boldsymbol{e}) = \frac{1}{2}\boldsymbol{e}^T\boldsymbol{e} \tag{73}$$

Using Eqs. (69) and (72), the derivative of the Lyapunov function is

$$\dot{V}_e = \boldsymbol{e}^T\dot{\boldsymbol{e}} = -\boldsymbol{e}^T[A][\tau]\boldsymbol{d} \tag{74}$$

After setting $\boldsymbol{d} = k_e\boldsymbol{e}$, where the scalar k_e is a positive, and making use of the properties $[A]\boldsymbol{e} = \boldsymbol{e}$ and $[\tau]^2 = [\tau]$, $\dot{V}_e$ is rewritten as

$$\dot{V}_e = -\boldsymbol{e}^T[\tau]^T[\tau]\boldsymbol{e} \leq 0 \tag{75}$$

which is negative semi-definite. Therefore, the VSCMG null motion

$$\dot{\boldsymbol{\eta}} = k_e\left[[I_{N\times N}] - [W][Q]^T\left([Q][W][Q]^T\right)^{-1}[Q]\right][A]\begin{pmatrix}\boldsymbol{\Omega}_f - \boldsymbol{\Omega} \\ \boldsymbol{\gamma}_f - \boldsymbol{\gamma}\end{pmatrix} \tag{76}$$

is a globally stable. Note, however, that no guarantee of asymptotic stability can be made. As is the case with the classical single-gimbal CMG null motion, it is still not possible to reorient between any two arbitrary sets of $\boldsymbol{\eta}$ vectors because the internal momentum vector must be conserved. If the momentum is not conserved, than some torque acts on the spacecraft.

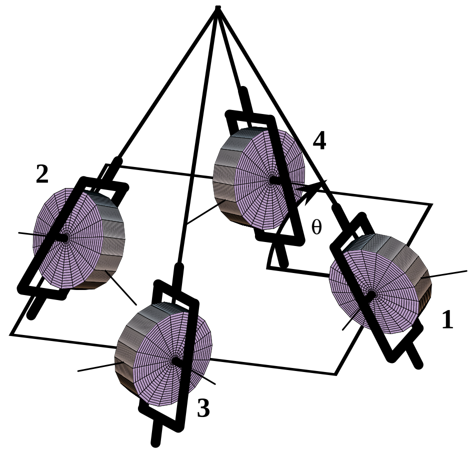

Figure 2: Four VSCMGs in a Pyramid Configuration

Numerical Simulations

Neglecting the VSCMG transverse and gimbal inertia effects not only simplifies the analysis and simulation, but only directly provides the correct control input $\dot{\boldsymbol{\gamma}}$ required by CMGs. However, including these small inertia terms and using the gimbal acceleration based steering law provides for a more accurate simulation. Also, the physical torques required by the RW and CMG torque motors can be obtained. Results for two simulations are presented in this section. The first simulation uses the gimbal velocity based steering law in Eq. (56) to study the desired performance. The second simulation uses the acceleration based steering law to verify that it does indeed track the velocity based steering law.

A rigid spacecraft with some initial body angular velocity $\boldsymbol{\omega}$ and non-zero attitude $\boldsymbol{\sigma}$ is to be brought to rest at a zero attitude vector. The $\boldsymbol{\sigma}$ vector is assumed to be measured from a desired attitude. Four equal VSCMGs are embedded in the spacecraft in a standard pyramid configuration as shown in Figure 2. All simulation parameters are shown in Table 1. The angular velocity feedback matrix $[P]$ is chosen to be of diagonal form with the entries shown in the table. The initial $\dot{\boldsymbol{\gamma}}$ value is only used in the gimbal acceleration based steering law.

The VSCMG steering laws are compared to the single-gimbal CMG steering laws presented by Oh and Vadali in Ref. 1. Their steering law combines the Singularity Robustness Steering Law (SRSL)

$$\dot{\boldsymbol{\gamma}} = [D_1]^T \left([D_1][D_1]^T + \alpha I_{3x3}\right)^{-1} \boldsymbol{L}_r \tag{77}$$

with a variable angular velocity feedback gain matrix $[P]$. The parameter α depends on the singularity index δ through

$$\alpha = \alpha_0 e^{-\delta} \tag{78}$$

The SRSL smoothly handles rank deficient $[D_1]$ matrices by having a slightly inaccurate matrix inverse. To escape situations where the orthogonality index $\mathcal{O}$ has gone to zero, the required torque is varied by changing the feedback gain matrix $[P]$ elements through

$$[P] = \begin{bmatrix} P_1 & -\delta P & \delta P \\ \delta P & P_2 & -\delta P \\ -\delta P & \delta P & P_3 \end{bmatrix} \tag{79}$$

where the smoothly varying parameter δP is related to the orthogonality factor through

$$\delta P = \begin{cases} \delta P_0 \frac{\mathcal{O}_0 - \mathcal{O}}{\mathcal{O}_0} & \text{for } \mathcal{O} < \mathcal{O}_0 \\ 0 & \text{for } \mathcal{O} \geq \mathcal{O}_0 \end{cases} \tag{80}$$

Table 1: VSCMG Simulation Parameters

Parameter	Value	Units
I_{s_1}	86.215	kg-m^2/sec
I_{s_2}	85.070	kg-m^2/sec
I_{s_3}	113.565	kg-m^2/sec
$\boldsymbol{\sigma}(t_0)$	[0.414 0.3 0.2]	
$\boldsymbol{\omega}(t_0)$	[0.01 0.05 − 0.01]	rad/sec
N	4	
θ	54.75	degrees
J_s	0.13	kg-m^2
J_t	0.04	kg-m^2
J_g	0.03	kg-m^2
$\gamma_i(t_0)$	[0 0 90 − 90]	deg
$\dot{\gamma}_i(t_0)$	[0 0 0 0]	rad
$\Omega(t_0)$	14.4	rad/sec
$[P]$	[13.13 13.04 15.08]	kg-m^2/sec
K	1.70	kg-m^2/sec^2
$K_{\dot{\gamma}}$	1.0	sec^{-1}
$W_{s_i}^0$	2.0	
W_{g_i}	1.0	
μ	10^{-9}	

The parameter $\mathcal{O}_0$ was set to 0.01 and δP_0 is 0.1. The comparison of the steering laws is not done to establish that one control law is necessarily better than the other. They both have different purposes. The modified SRSL method is included because it illustrates the inherent problems of classical single-gimbal CMG steering laws and how they temporarily may not be able to provide the required torque. The VSCMG steering law is designed to *always* provide the required torque. However, as will be seen in the following simulation results, this does come at a price of increased energy consumption.

The first simulation utilizes the VSCMG steering law in Eq. (56). As a comparison, the results of using the modified SRSL in Ref. 1 are included too and are indicated by the dashed lines in Fig. 3. Having the third and fourth VSCMG gimbal angles be initially +90 and -90 degrees each makes the determinant δ zero at the beginning of the simulation as is shown in Figure 3.i. The determinant becomes nonzero for a few seconds and then goes back to zero for a while. About 18 seconds into the maneuver, the determinant becomes nonzero for the VSCMG steering law and then remains nonzero for the entire maneuver duration of 500 seconds. The standard CMG steering law has a similar behavior initially, but never becomes nonzero again after dipping back to zero at 5 seconds into the maneuver. The reason for this is seen by studying the orthogonality index $\mathcal{O}$ in Figure 3.ii. The index $\mathcal{O}$ is nonzero to begin with, allowing the CMG steering law to provide some torque onto the spacecraft. However, as the δ becomes zero again $\mathcal{O}$ also goes to zero for the CMG steering law, while the VSCMG steering law retains a nonzero $\mathcal{O}$ throughout the maneuver. The modified feedback gain matrix $[P]$ does change $\boldsymbol{L}_r$ sufficiently that the spacecraft does approach the desired attitude as is shown in Figure 3.iii. However, this occurs very slowly. Here is a situation where the classical CMG steering law effectively remains trapped near a singular configuration which results in a very degraded performance. On the other hand, both the attitude and body angular velocity decay as described by the feedback law for the VSCMG as shown in Figures 3.iii and 3.iv. If it were essential for the mission that the spacecraft would actually follow the prescribed trajectory, the results of the classical CMG steering law clearly would be unsatisfactory, while the VSCMG steering law stays right on track.

Figures 3.v and 3.vi show the gimbal angles and gimbal angle rate time histories. For both the

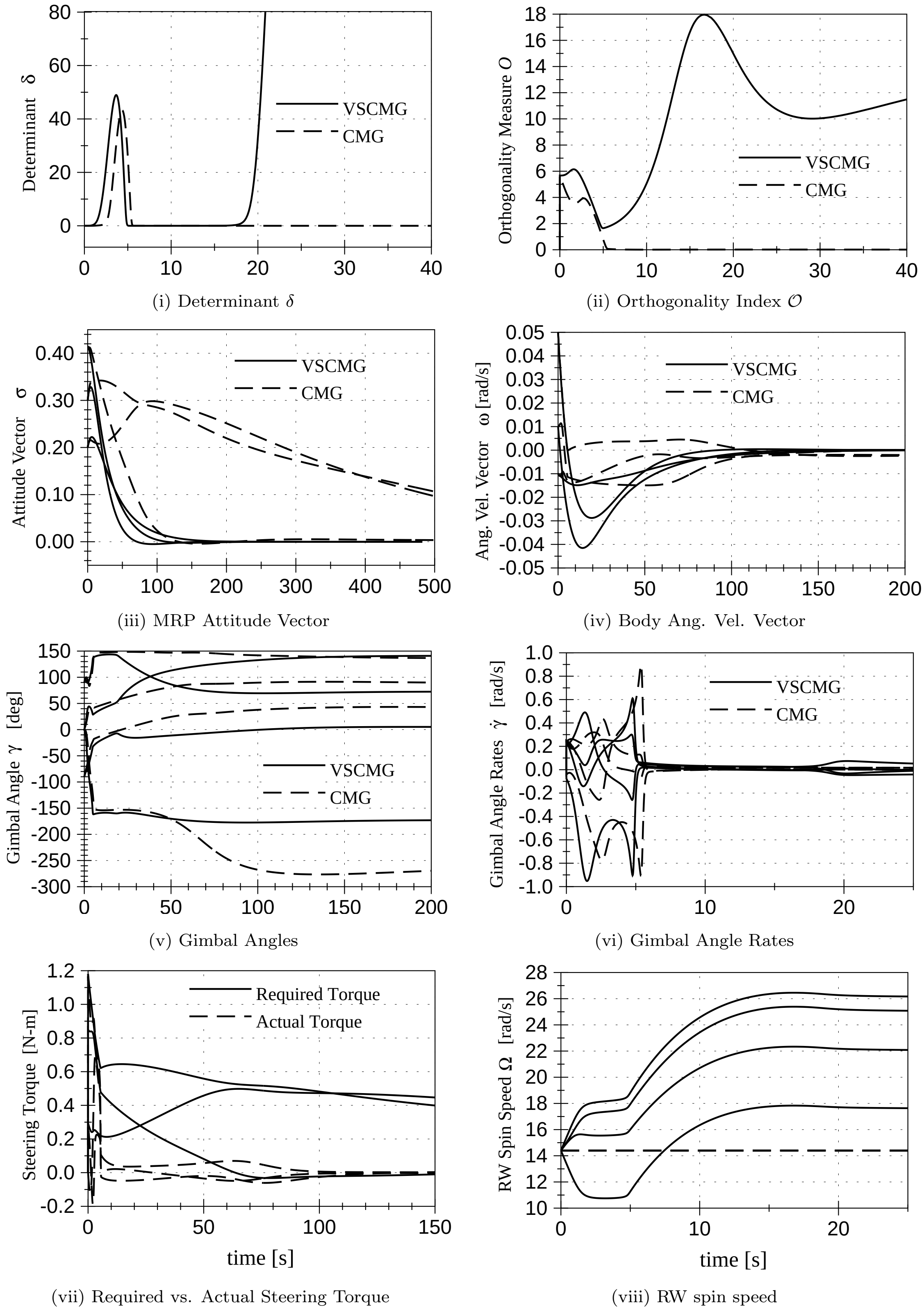

(i) Determinant δ

(ii) Orthogonality Index $\mathcal{O}$

(iii) MRP Attitude Vector

(iv) Body Ang. Vel. Vector

(v) Gimbal Angles

(vi) Gimbal Angle Rates

(vii) Required vs. Actual Steering Torque

(viii) RW spin speed

Figure 3: Gimbal Velocity Based Steering Law Simulation

VSCMG and CMG steering law the gimbal rates are relatively large at the beginning of the maneuver where the CMGs remain close to a singular configuration. After about 6 seconds the CMG rates remain almost zero because the steering law is essentially "entrapped" in the singular configuration. Figure 3.vii compares the required torque $\boldsymbol{L}_r$ to the actual torque $\boldsymbol{L}_a$ produced by the CMG steering law. The VSCMG actual torque is not shown in this figure because it is always equal to $\boldsymbol{L}_r$. While having the SRSL and the time varying $[P]$ matrix to help the standard CMG steering law and this spacecraft would eventually reach the desired target state, this Figure shows clearly that the actual torque produced at several time segments much less than the required torque. However, for the VSCMG steering law to keep the spacecraft on track comes at the expense of spinning the RW up or down on occasion. The RW spin speeds $\boldsymbol{\Omega}$ are shown in Figure 3.viii. The RW mode is employed twice when the determinant δ goes to zero. Once the CMGs are away for a singular configuration, the spin speeds remain essentially constant.

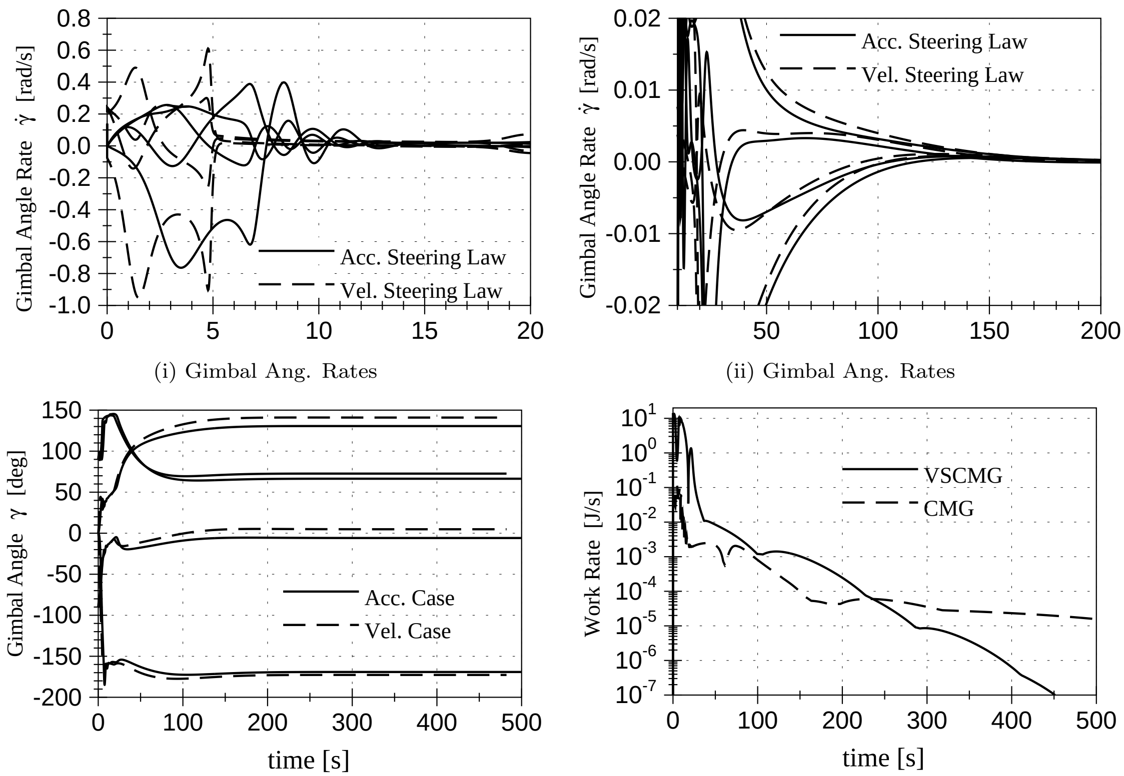

(i) Gimbal Ang. Rates

(ii) Gimbal Ang. Rates

(iii) Gimbal Angles

(iv) Work Rates

Figure 4: Gimbal Acceleration Based Steering Law Simulation

The second simulation uses the gimbal acceleration based steering law in Eq. (68) and the results are shown in Figure 4. The gimbal acceleration were designed such that they would provide the same performance as the velocity based steering law. Figures 4.i and 4.ii show the gimbal angle rates for both the gimbal acceleration and velocity based steering laws. As expected, during the initial phase of the maneuver the two gimbal rates are quite different as seen in Figure 4.i. This is because the initial gimbal rates were set to zero and were not equal to the desired gimbal rates from Eq. (56). However, as Figure 4.ii shows clearly, after about 10 to 20 seconds into the maneuver, the gimbal rate performance of the acceleration steering approaches that of the desired velocity based steering law. The corresponding gimbal angles for both cases are shown in Figure 4.iii.

The natural drawback to using the RW modes of the VSCMG to maneuver through classical CMG singularities is evident when studying the work rate of the VSCMG steering law compared to the standard CMG steering law in Figure 4.iv. The work rate $\dot{W}$ for the VSCMGs is defined as

$$\dot{W} = \sum_{i=1}^{N} |\Omega_i u_{s_i}| + |\dot{\gamma}_i u_{g_i}| \tag{81}$$

During the initial phase of the maneuver, where the determinant δ is very small, the energy consumption to drive the RW modes is relatively large compared to the CMG modes. Away from this singularity, the energy consumption is very comparable to that of the CMG steering law. The power of RW torques is typically the limiting factor for the VSCMG devices to decide on how large a structure they could be used. However, for smaller spacecraft which may be able to afford temporary RW modes, the VSCMG steering law provides interesting possibilities. Other authors have looked into augmenting CMG cluster with thrusters to keep the spacecraft on track during near singular configurations. Using the RW modes has several benefits over using thrusters. They provide a much smoother response compared to using thrusters and will excite few flexible modes within the spacecraft. Also, RW don't require propellant to operate, but use electrical power which can be readily recharged from solar arrays.

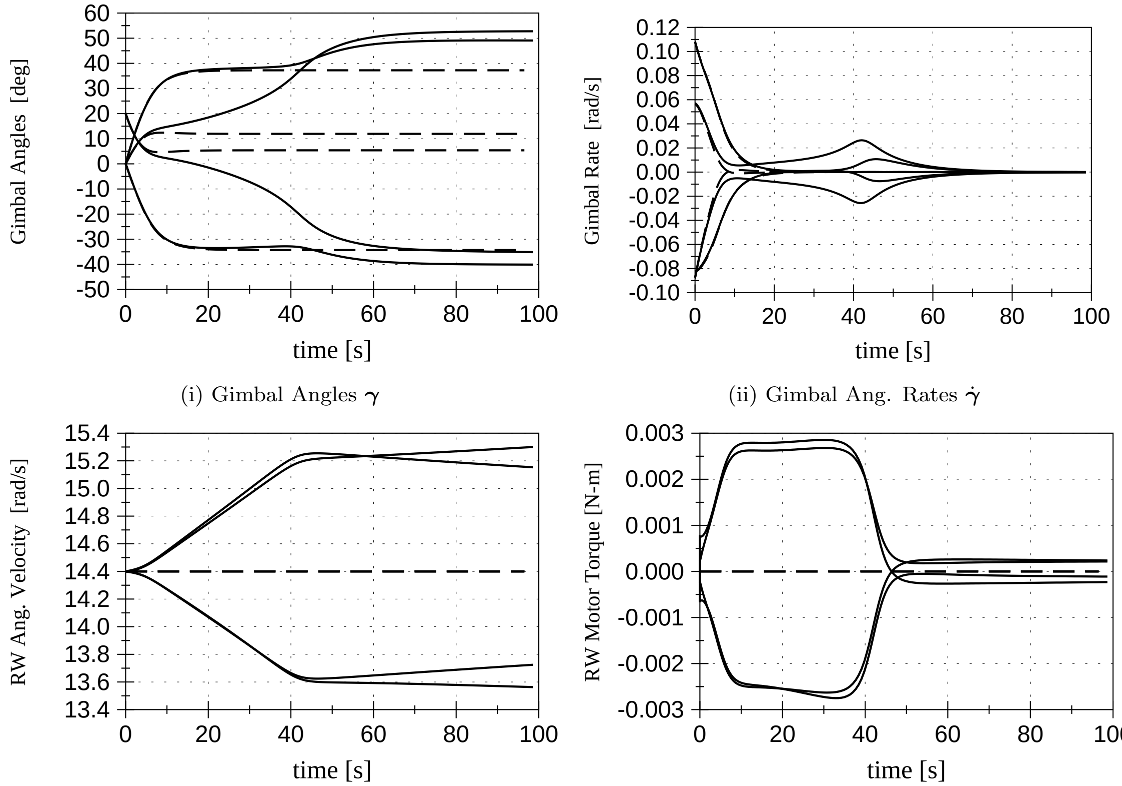

(i) Gimbal Angles $\boldsymbol{\gamma}$

(ii) Gimbal Ang. Rates $\dot{\boldsymbol{\gamma}}$

(iii) RW Spin Speeds $\boldsymbol{\Omega}$

(iv) RW Motor Torques $\boldsymbol{u}_s$

Figure 5: Reconfiguring the CMG Gimbals using VSCMG Null Motion

The third simulation shown in Figure 5 illustrates the use of the VSCMG null motion to reorient the CMGs to a set of preferred gimbal angles where the final $\boldsymbol{\Omega}$ was irrelevant (i.e. $a_{RW} = 1$ and $a_{CMG} = 1$). The initial and preferred gimbal angles are $(0, 0, 0, 20)$ degrees and $(45, 45, -45, -45)$ degrees respectively. The scalar k_e was set to 0.1 and the weights W_{s_i} were held constant at 2. Note that this gimbal angle reconfiguration cannot be performed with the classical CMG null motion where $\boldsymbol{\Omega}$ is held constant, because the initial configuration has an internal momentum vector and the preferred configuration would have none. The performance of the classical CMG null motion is shown in Figure 5 through dashed lines. Figure 5.i clearly shows that the VSCMG null motion is able to reconfigure the $\boldsymbol{\gamma}$ much closer to $\boldsymbol{\gamma}_f$ than the CMG null motion. The corresponding gimbal rates $\dot{\boldsymbol{\gamma}}$, shown in Figure 5.ii, are smooth and remain relatively small compared to the maximum allowable gimbal rates of 2 rad/s. The VSCMGs achieve this feat by varying the RW spin speeds. However, as shown in Figure 5.iii, they do not have to be changed much to prevent a torque being applied onto the spacecraft. The corresponding torque required by the RW motors is shown in Figure 5.iv. The magnitude of these torques are of the same order as the RW torques required by the classical CMG to maintain a constant $\boldsymbol{\Omega}$ during a spacecraft reorientation. Therefore, *no hardware change* would be required to use the VSCMG null motion to reconfigure the gimbal angles, only a change in the feedback control law of the RW speeds.

Another simulation was performed where the initial gimbal angles were $(0, 0, 0, 0)$ degrees as was done in Ref. 23. Note that this reconfiguration can be accomplished with CMG null motion because the initial and final configuration has the same internal momentum vector. The VSCMG null motion was identical to the CMG null motion where $\boldsymbol{\Omega}$ was held constant even though W_{s_i} was held constant at 2. The minimum norm inverse automatically used the more efficient CMG mode here.

Besides reorienting the gimbals with the VSCMG null motion, it is also possible to change the RW spin speeds $\boldsymbol{\Omega}$ to desired values by setting $a_{RW} = 1$. The extra degrees of control allow the internal momentum vector to be redistributed across the CMG and RW modes in an infinity of ways. A limiting factor in how fast this reconfiguring can be done is the typically the maximum allowable RW motor torques. The speed of the VSCMG null motion is directly control by the size of k_e.

Conclusions

The equations of motion of a rigid spacecraft with N VSCMGs embedded are introduced, including the physical control torques required by the gimbal and the RW motors. A globally asymptotically stable feedback control law based on Lyapunov theory is developed to stabilize the spacecraft at a given attitude. The velocity based steering law contains a weighted minimum norm inverse. The RW mode weights depend on the proximity of the gimbal frame to a classical single-gimbal CMG singularity. Away from such a singularity the RW mode weights are essentially zero and the VSCMG performs like a CMG. Close to a singularity the CMG mode is augmented with the RW mode to ensure that the required torque $\boldsymbol{L}_r$ is always precisely produced. An acceleration based steering law is also presented that will yield the desired velocity based steering law performance and allows for work rate studies. Further, the use of the VSCMG null motion to reconfigure the gimbal angles and RW speeds is presented. The gimbal angles are able to be reoriented in a much more general manner than was possible with the CMG null motion, thus making it easier to avoid singularities altogether. The resulting torques required of the RW motors are typically well within the current capabilities of single-gimbal CMG reaction wheel motors. Therefore, utilizing the VSCMG null motion in this manner would only require a change the RW feedback law and not necessary a hardware redesign.

References

[1] H. S. Oh and S. R. Vadali. "Feedback Control and Steering Laws for Spacecraft Using Single Gimbal Control Moment Gyros," *Journal of the Astronautical Sciences*, Vol. 39, No. 2, April–June 1991, pp. 183–203.

[2] B. R. Hoelscher and S. R. Vadali. "Optimal Open-Loop and Feedback Control Using Single Gimbal Control Moment Gyroscopes," *Journal of the Astronautical Sciences*, Vol. 42, No. 2, April–June 1994, pp. 189–206.

[3] S. Krishnan and S. R. Vadali. "An Inverse-Free Technique for Attitude Control of Spacecraft Using CMGs," *Acta Astronautica*, Vol. 39, No. 6, 1997, pp. 431–438.

[4] N. S. Bedrossian. *Steering Law Design for Redundant Single Gimbal Control Moment Gyro Systems.* M.S. Thesis, Mechanical Engineering, MIT, Aug. 1987.

[5] J. L. Junkins and J. D. Turner. *Optimal Spacecraft Rotational Maneuvers.* Elsevier Science Publishers, Amsterdam, Netherlands, 1986.

[6] H. Schaub, R. D. Robinett, and J. L. Junkins. "Globally Stable Feedback Laws for Near-Minimum-Fuel and Near-Minimum-Time Pointing Maneuvers for a Landmark-Tracking Spacecraft," *Journal of the Astronautical Sciences*, Vol. 44, No. 4, Oct.–Dec. 1996, pp. 443–466.

[7] K. Ford and C. D. Hall. "Flexible Spacecraft Reorientations Using Gimbaled Momentum Wheels," *AAS/AIAA Astrodynamics Specialist Conference*, Sun Valley, Idaho, August 1997. Paper No. 97-723.

[8] D. T. Greenwood. *Principles of Dynamics*. Prentice-Hall, Inc, Englewood Cliffs, New Jersey, 2nd edition, 1988.

[9] W. E. Wiesel. *Spaceflight Dynamics*. McGraw-Hill, Inc., New York, 1989.

[10] H. S. Oh, S. R. Vadali, and J. L. Junkins. "On the Use of the Work-Energy Rate Principle for Designing Feedback Control Laws," *AIAA Journal of Guidance, Control and Dynamics*, Vol. 15 No. 1, Jan–Feb 1992, pp. 272–277.

[11] H. Schaub and J. L. Junkins. "Stereographic Orientation Parameters for Attitude Dynamics: A Generalization of the Rodrigues Parameters," *Journal of the Astronautical Sciences*, Vol. 44, No. 1, Jan.–Mar. 1996, pp. 1–19.

[12] P. Tsiotras, J. L. Junkins, and H. Schaub. "Higher Order Cayley Transforms with Applications to Attitude Representations," *Journal of Guidance, Control and Dynamics*, Vol. 20, No. 3, May–June 1997, pp. 528–534.

[13] P. Tsiotras. "Stabilization and Optimality Results for the Attitude Control Problem," *Journal of Guidance, Control and Dynamics*, Vol. 19, No. 4, 1996, pp. 772–779.

[14] T. F. Wiener. *Theoretical Analysis of Gimballess Inertial Reference Equipment Using Delta-Modulated Instruments*. Ph.D. dissertation, Department of Aeronautics and Astronautics, Massachusetts Institute of Technology, March 1962.

[15] S. R. Marandi and V. J. Modi. "A Preferred Coordinate System and the Associated Orientation Representation in Attitude Dynamics," *Acta Astronautica*, Vol. 15, No. 11, 1987, pp. 833–843.

[16] M. D. Shuster. "A Survey of Attitude Representations," *Journal of the Astronautical Sciences*, Vol. 41, No. 4, 1993, pp. 439–517.

[17] H. Schaub, P. Tsiotras, and J. L. Junkins. "Principal Rotation Representations of Proper NxN Orthogonal Matrices," *International Journal of Engineering Science*, Vol. 33, No. 15, 1995, pp. 2277–2295.

[18] J. L. Junkins and Y. Kim. *Introduction to Dynamics and Control of Flexible Structures*. AIAA Education Series, Washington D.C., 1993.

[19] R. Mukherjee and D. Chen. "Asymptotic Stability Theorem for Autonomous Systems," *Journal of Guidance, Control, and Dynamics*, Vol. 16, Sept.–Oct. 1993, pp. 961–963.

[20] R. Mukherjee and J. L. Junkins. "Invariant Set Analysis of the Hub-Appendage Problem," *Journal of Guidance, Control, and Dynamics*, Vol. 16, Nov.–Dec. 1993, pp. 1191–1193.

[21] J. L. Junkins. *An Introduction to Optimal Estimation of Dynamical Systems*. Sijthoff & Noordhoff International Publishers, Alphen aan den Rijn, Netherlands, 1978.

[22] Y. Nakamura and H. Hanafusa. "Inverse Kinematic Solutions with Singularity Robustness for Robot Manipulator Control," *Journal of Dynamic Systems, Measurement, and Control*, Vol. 108, Sept. 1986, pp. 164–171.

[23] S. R. Vadali, H. S. Oh, and S. R. Walker. "Preferred Gimbal Angles for Single-Gimbal Control Moment Gyros," *Journal of Guidance, Control and Dynamics*, Vol. 13, No. 6, Nov.–Dec. 1990, pp. 1090–1095.